cartographic longitude of 2.60° ± 0.63°, 2.3σ from the actual location given by the ephemeris. We consider this not only a satisfactory agreement, but also an excellent check on the Doppler-determined gravity. The value of C_{22} in the system of rotated axes is $(C_{22}^2 + S_{22}^2)^{1/2}$, and S_{22} is zero by definition. The axis rotation increases C_{22} to 131.5 ± 2.5 × 10^{-6} and μ is reduced from 0.993 to 0.988.

11. Our best estimate for Europa's *GM* is 3202.72 ± 0.05 km^3 s^{-2}. Using the best current values for *G* and *R* (*4*), we obtain a mass for Europa of 4.79982 (±0.00062) × 10^{22} kg and a mean density of 2989 ± 46 kg m^{-3}. The rotational parameter $q_r = \omega^2 R^3/GM$ is 5.019 (±0.077) × 10^{-4}, where the angular velocity $\omega = 2\pi/P$ is determined from Europa's sidereal orbital period P = 3.551 days [P. K. Seidelmann, *Explanatory Supplement to the Astronomical Almanac* (University Science Books, Mill Valley, CA, 1992)]. The errors in the density and q_r are dominated by the 8-km error in Europa's radius.
12. The gravity coefficient C_{22} = 131.5 × 10^{-6} and the rotational parameter q_r = 5.019 × 10^{-4} can also be used to compute the equilibrium shape of the Roche-Darwin ellipsoid (*6*). In terms of the principal axes ($c < b < a$), where *a* is the equatorial radius, *c* is the polar radius, and *b* is the intermediate radius, the polar flattening is $(a - c)/c$ = 2.056 × 10^{-3}. The distortion of the equatorial cross section can be expressed by the parameter $(b - c)/(a - c)$, which according to equilibrium theory is exactly 1/4. We use the axial moment of inertia *C* normalized to MR^2 as a constraint on the interior models. We ignore the small differences between the three principal moments (~0.1%).
13. G. Schubert, T. Spohn, R. T. Reynolds, in *Satellites*, J. A. Burns and M. S. Matthews, Eds. (Univ. of Arizona Press, Tucson, 1986), pp. 629–688; M. H. Carr *et al.*, *Nature* **391**, 363 (1998); R. T. Pappalardo *et al.*, *ibid.*, p. 365; P. E. Geissler *et al.*, *ibid.*, p. 368; R. Sullivan *et al.*, *ibid.*, p. 371.
14. M. G. Kivelson *et al.*, *Science* **276**, 1239 (1997).
15. K. K. Khurana *et al.*, *Nature*, in press.
16. J. D. Anderson, W. L. Sjogren, G. Schubert, *Science* **272**, 709 (1996).
17. Because Europa and the moon are similar in size and density, the expected temperature in an undifferentiated Europan mantle—produced by radiogenic heating, subsolidus convective heat transport, and temperature-dependent mantle viscosity—can be estimated from calculations carried out for the lunar interior. Lunar calculations are reported in G. Schubert, R. E. Young, P. Cassen, *Philos. Trans. R. Soc. London Ser. A* **285**, 523 (1977). The deep mantle temperature in these lunar models is between 1500 and 1600 K.
18. P. Ulmer and V. Trommsdorff, *Science* **268**, 858 (1995).
19. R. Woo and J. W. Armstrong, *J. Geophys. Res.* **84**, 7288 (1979).
20. This work was sponsored by the Galileo Project and was performed at the Jet Propulsion Laboratory, California Institute of Technology, under contract with NASA. G.S. and W.B.M. acknowledge support by grants from NASA through the Galileo Project at JPL and the Planetary Geology and Geophysics program.

6 May 1998; accepted 4 August 1998

Origin of Multikilometer Earth- and Mars-Crossing Asteroids: A Quantitative Simulation

Fabio Migliorini,* Patrick Michel, Alessandro Morbidelli,† David Nesvorný, Vincenzo Zappalà

Orbital dynamic simulations show that many asteroids in the main asteroid belt are driven toward Mars-crossing orbits by numerous weak mean motion resonances, which slowly increase the orbital ellipticity of the asteroids. In addition, half of the Mars-crossing asteroids (MCAs) transition to Earth-crossing asteroids (ECAs) in less than 20 million years. This scenario quantitatively explains the observed number of large ECAs and MCAs.

Most ECAs and MCAs are fragments of larger main belt asteroids. According to the classic scenario (*1*), they were injected by the collisions that formed them into a resonance (*2*), which increased their eccentricities until they started to cross the terrestrial planets' orbits. The encounters with the planets then spread them all over the region where they are now observed and categorized as ECAs or MCAs (*3*).

Recent simulations (*4*) showed that the median dynamical lifetime of bodies initially placed in the 3/1 or ν_6 resonances is only 2 My (million years), because these resonances pump the eccentricity to unity, forcing most of the resonant bodies to collide with the sun. As a consequence, in order to sustain the observed planet-crossing population in steady state, the number of bodies injected into resonance per million year would need to be about 25% of the total population. This indicates that the classic scenario cannot explain the origin of multikilometer ECAs and MCAs. In fact, 10 ECAs and 354 MCAs with diameters larger than 5 km are currently known (*5*) despite the fact that bodies of this size can be injected into resonance only during very energetic and rare breakup events, such as those leading to formation of asteroid families (*6*). Also, the classic scenario would predict a lower MCA/ECA ratio than is observed because asteroids in the 3/1 and ν_6 resonances experience such a rapid increase in their eccentricity that they quickly become ECAs or graze the sun before encounters with Mars can extract the asteroids from these resonances into MCAs.

The orbital distribution of MCAs consists of four groups—hereafter denoted by MB, MB2, HU, and PH—with values of semimajor axis *a* and inclination *i* similar to those of four populations of non–planet-crosser asteroids: the main belt below the ν_6 resonance, the main belt above the ν_6 resonance and beyond 2.5 AU, the Hungarias, and the Phocaeas. This similarity suggests that these populations continuously lose objects to the MCA region due to an increase in eccentricity, sustaining the MB, HU, and PH groups. Only 2% of MCAs larger than 5 km have *a* and *i* different from those non–planet-crosser asteroids and therefore must have evolved relative to the orbit they had when they first crossed the orbit of Mars: we denote them EV (Fig. 1).

To better understand the process by which non–planet-crossing asteroids become MCAs, and in particular the dynamical link between the main belt and MB populations, we have numerically integrated (*7*) the evolution of 412 main belt asteroids, a representative sample of the population with a = 2.1 to 2.5 AU, $i < 15°$, perihelion distance $q < 1.8$ AU and not intersecting the orbit of Mars during the first 300,000 years. The integrations covered a time span of 100 My, along which we numerically computed the time evolution of proper elements to distinguish between regular and chaotic asteroids (*8*).

Integrations show that the majority of the asteroids are on chaotic orbits and 25% of them become MBs (Fig. 2). We find that this process is mainly due to mean motion resonances with Mars (3/5, 7/12, 4/7, 5/9, 7/13, and 1/2), mean motion resonances with Jupiter (7/2 and 10/3), and three-body mean motion resonances between Jupiter, Saturn, and the asteroid or Mars, Jupiter, and the asteroid (*9*). Although the most important source region of MBs is the one with $a < 2.17$ AU, where high-order mean motion resonances with Mars are particularly dense, in practice, asteroids are removed from the main belt all over the 2.1- to 2.5-AU range, driven by numerous weak mean motion resonances. It is possible that a similar process also drives Hungaria and Phocaea asteroids to Mars-crossing orbits, sustaining the HU and PH populations.

To quantify the exchange of asteroids among non–planet-crossers, MCAs and ECAs, we have also integrated the evolution of 511 MCAs, a representative sample of their total population. MCAs become ECAs

F. Migliorini, Armagh Observatory, College Hill BT61 9DG, Northern Ireland, United Kingdom, and Osservatorio Astronomico di Torino, I-10025 Pino Torinese, Italy. P. Michel, Osservatorio Astronomico di Torino, I-10025 Pino Torinese, Italy, and Observatoire de la Côte d'Azur, B.P. 4229, 06304 Nice cedex 4, France. A. Morbidelli and D. Nesvorný, Observatoire de la Côte d'Azur, B.P. 4229, 06304 Nice cedex 4, France. V. Zappalà, Osservatorio Astronomico di Torino, I-10025 Pino Torinese, Italy.

*Died on 2 November 1997 in a mountain accident. The paper is devoted to his memory.

†To whom correspondence should be addressed. E-mail: morby@obs-nice.fr

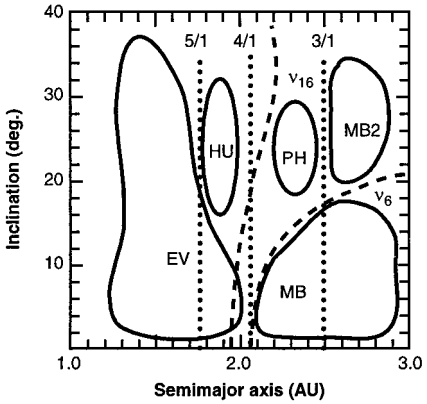

Fig. 1. Schematic representation of the MCA distribution. Dashed curves denote location of ν_6 and ν_{16} secular resonances; dotted lines correspond to positions of the 5/1, 4/1, and 3/1 mean motion resonances with Jupiter. Solid contours sketch bounds of MCA subpopulations.

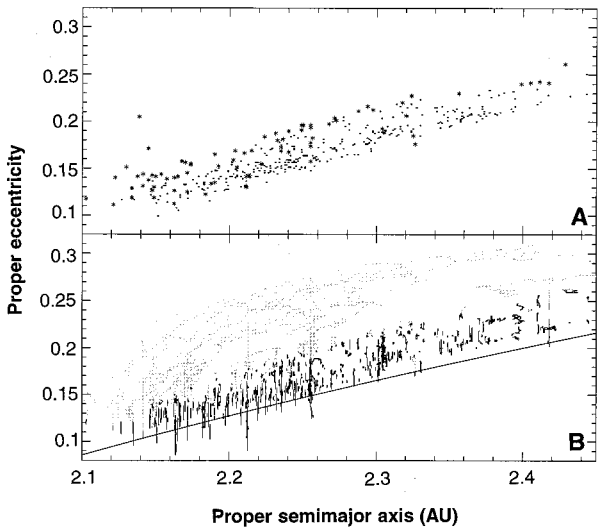

Fig. 2. Origin of MBs from the main belt. (**A**) Initial proper semimajor axis and eccentricity of integrated asteroids. Asterisks denote the bodies that will become Mars crossers within the integration time span. (**B**) Trace left by their time evolution. Proper elements are constant for regular asteroids, whose orbital elements have quasi-periodic evolution, and change over time for those evolving chaotically. If all asteroids were regular, (B) and (A) would be identical, so comparison of the two plots allows us to appreciate that most of the asteroids chaotically migrate in the proper element plane. Before becoming MCAs (black), asteroids migrate in proper eccentricity, keeping the proper semimajor axis close to its initial value. While the asteroids are MCAs (gray), they migrate in proper semimajor axis as a result of close encounters with Mars, which force them to evolve along curves of quasi-constant Tisserand invariant (*17*). The transfer to Earth-crossing orbits happens in most cases when the MCAs enter the 3/1 or ν_6 resonances (both of which are outside the semimajor axis range plotted here). Solid curve denotes proper perihelion distance equal to 1.92 AU.

by random walking in a semimajor axis under the effects of close encounters with Mars until entering into some resonance that increases the eccentricity to within the ECA range (*10*). The median time to become an ECA is about 20 My for MBs, and it is longer for HUs and PHs because of the reduced strength of martian encounters at large inclinations. The MBs are also the Mars-crossing population with the shortest dynamical lifetime (about 25 My); their most typical end states are collision with the sun or ejection beyond Saturn's orbit (Table 1).

Our simulation of what happens to an initial population of MCAs allows us to determine the number of bodies in ECA or EV orbits as a function of time. We scale the number of bodies down to reflect the results we would expect if we had started with the actual number of MCAs with diameters >5 km (*11*). The number of ECAs larger than 5 km evolved from the initial MB, HU, and PH populations increases rapidly with time, because a fraction of the MB population (those members having $q \sim 1$ AU or who are rapidly captured into 3/1 or ν_6 resonance) becomes ECA on a short time scale (Fig. 3A). Then, between 15 and 60 My the number of ECAs oscillates mainly between 5 and 10 bodies, with an average of 7 bodies. Finally, the number of bodies slowly decays because of the 25 My dynamical half-life of the MB population. Four to five objects with diameters greater than 5 km are sustained on orbits typical of EVs between 20 and 60 My, with equal contributions from the MB and HU populations (Fig. 3B). The dynamical paths of EVs from MBs and HUs are different. MBs first become ECAs and then decrease their semimajor axis below 2 AU due to encounters with Earth and Venus, where the eccentricity temporarily decreases under the effect of some resonance (*12*), raising the perihelion distance above the ECA limit. Few MBs become EVs without first being ECAs. Conversely, HUs become EVs by decreasing their inclination, because of the proximity of the ν_{16} resonance (*13*). Few HUs become ECAs without first being EVs.

The real numbers of bodies sustained on

Table 1. Statistics of MCA evolutions. Each class of objects is defined by its label. EV are crossing asteroids either having current semimajor axis $a < 1.77$ AU (location of the 5/1 resonance with Jupiter) or $1.77 < a < 2.06$ AU (between the 5/1 and 4/1 resonances with Jupiter) and inclination $i < 15°$. MBs are MCAs with $a > 2.06$ AU (location of the 4/1 resonance with Jupiter) and an inclination such that they are below the ν_6 secular resonance; HUs have $1.77 < a < 2.06$ AU and $i > 15°$; PHs have $2.1 < a < 2.5$ AU (between the 4/1 and 3/1 resonances with Jupiter) and are situated above the ν_6 secular resonance; MB2s have $a > 2.5$ AU and are situated above the ν_6 secular resonance. Diameters are estimated assuming different albedos: 0.2 for EV asteroids and 0.3 for HU ones (taking into account that most are bright E-type asteroids); they are 0.16 to 0.08 (depending on the semimajor axis) for the other classes (*18*). The number of integrated bodies, the time spans covered by the integrations, and the number of bodies that are ejected beyond Saturn or impact the sun (in parentheses the percentage that they represent over the number of nonsurviving bodies) are shown. Time scales are shown for 50% (half-life) and 90% decay of the integrated bodies and median times T_{cr} for crossing the orbits of Earth and Venus. The number (percentage) of objects that are temporarily in regions of particular interest and the median time spent in these regions (T_{med}) are listed. *Q* indicates aphelion distance.

	EV	MB	HU	PH	MB2
Total No. of bodies	105	1039	114	165	37
No. with $D > 5$ km (%)	7 (6.67)	240 (23.1)	17 (14.9)	78 (47.3)	12 (32.4)
No. of integrated bodies	53	322	56	66	14
Length (My)	147	200	147	200	200
Outside Saturn (%)	7 (17.1)	76 (25.4)	2 (6.9)	2 (6.4)	5 (41.7)
Impact sun (%)	26 (63.4)	205 (68.6)	25 (86.3)	28 (90.4)	6 (50.0)
Half-life (My)	93.0	23.7	137.2	>200	41.2
90% decay (My)	>147	114.2	>147	>200	144.7
No. of EC (%)	49 (92.5)	297 (92.2)	43 (76.8)	31 (47.0)	12 (85.7)
T_{cr} Earth (My)	11.6	19.1	74.6	>200	24.3
No. of VC (%)	43 (81.1)	285 (88.5)	36 (64.3)	31 (47.0)	12 (85.7)
T_{cr} Venus (My)	25.4	20.0	86.0	>200	25.2
Ever have $a < 2$ AU (%)	53 (100)	109 (33.4)	55 (98.2)	14 (21.2)	0
T_{med} (My)	72.4	6.5	105.7	6.2	—
Ever have $a < 1$ AU (%)	13 (24.5)	16 (5.0)	3 (5.4)	1 (1.5)	0
T_{med} (My)	12.7	10.7	10.2	8.3	—
Ever have $Q < 2$ AU (%)	45 (84.9)	29 (9.0)	33 (58.9)	1 (1.5)	0
T_{med} (My)	30.7	11.0	20.5	15.4	—

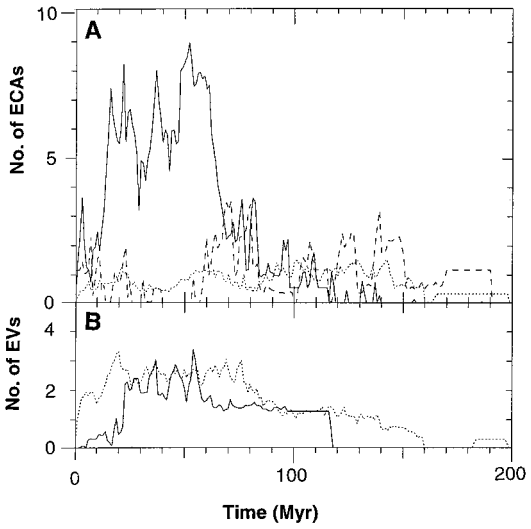

Fig. 3. (**A**) Number of bodies with a diameter larger than 5 km expected on ECA orbit starting from the present MBs (solid line), HUs (dotted line), and PHs (dashed line). (**B**) Same as (A) but for the number of expected EVs. The contribution of PHs is negligible.

ECA and EV orbits by the MB, HU, and PH populations depend on the number of MB, HU, and PH bodies supplied by the objects from the main belt, Hungaria, and Phocaea regions. To be in steady state, half the MB population should be regenerated every 25 My. In that case, a low estimate of the average steady-state populations of ECAs and EVs can be obtained by adding to their average number in the 25- to 50-My range (seven and five bodies, respectively) (Fig. 3) half the average numbers supplied by the MB population during the first 25 My (two and one bodies, respectively). The resulting populations are similar to those currently observed (10 ECAs and 7 EVs), showing that the MBs, HUs, and PHs are sufficient to sustain ECAs and EVs. Extinct comets and asteroid fragments, collisionally injected into the main resonances of the main belt, are not required to provide significant contributions to the ECA population (*14*).

The number of MBs larger than 5 km in the 2.1- to 2.5-AU range is 183. Because of their half-life, 91 of these asteroids should be dynamically eliminated in 25 My. Of the original main belt asteroids that we have integrated, 17% become MBs within 25 My. Because there are 263 asteroids larger than 5 km in the main belt region represented by our initial population, we estimate that 44 asteroids are resupplied to the MB population. However, the chaotic process that leads to the origin of MCAs concerns basically all the asteroids with a proper perihelion distance smaller than 1.92 AU (Fig. 2). According to the 1994 update of the proper elements catalog (*15*), about 1000 asteroids larger than 5 km in diameter in the inner belt have proper perihelion distances smaller than this threshold, including parts of the Flora and the Nysa families. In summary, there is a strong presumption that chaotic evolution in the inner asteroid belt will ensure the existence of the next generation of MB Mars crossers with $a < 2.5$ AU.

Sustaining the MB population on time scales longer than 25 My is problematic. In our integrations, after the first 10 My, the fastest transporting resonances are mostly depleted of objects, so that the escape process from the inner main belt becomes dominated by the action of the weakest resonances and consequently the escape rate decreases to an almost constant value of 10% of the population every 100 My. This rate would supply the MB population with about 100 bodies per 100 My, which seems to be insufficient to keep it in steady state. However, this result probably means that our simulation is too simplistic to describe the real evolution of the asteroidal populations on a 100-My time scale. Collisional processes, generating new multikilometer bodies on this time scale, should be taken into account as well as nonconservative dynamical phenomena, which allow the mobility of the proper semimajor axis of the asteroids in the main belt.

In past epochs, keeping the MBs in steady state during the last 3 Gy requires the escape of 12,000 asteroids larger than 5 km from the main belt. This is comparable to the number of bodies larger than 5 km that are estimated to currently exist with $a < 2.5$ AU in the main belt (*16*). It might not be a coincidence that the distribution of asteroids with respect to proper perihelion distance peaks at 1.95 AU. Chaotic diffusion could have substantially eroded the part of the main belt with proper $q < 1.95$ AU, providing generations of MCAs and ECAs throughout the history of the solar system.

References and Notes

1. See, for instance, R. Greenberg and M. Nolan, in *Asteroids II*, R. Binzel, T. Gerhels, M. S. Matthews, Eds. (Univ. of Arizona Press, Tucson, AZ, 1989), pp. 778–804.
2. Mainly the 3/1 mean motion resonance with Jupiter, which occurs when the orbital period of the asteroid is equal to 1/3 the Jovian period, or the ν_6 secular resonance, which occurs when the mean precession rate of the asteroid's perihelion equals that of Saturn. These are by far the most efficient resonances for the transport of bodies to large eccentricities.
3. For a list of ECAs and MCAs with perihelion distance < 1.3 AU (classically defined as Amors asteroids), see http://cfa-www.harvard.edu/iau/lists/Unusual.html.
4. B. J. Gladman *et al.*, *Science* **277**, 197 (1997).
5. Here ECAs are defined as the asteroids with perihelion and aphelion distance smaller and larger, respectively, than 1 AU, whereas MCAs are defined as those that are not currently Earth crossers and intersect the orbit of Mars within one precession cycle of their orbit. To identify all MCAs, we have integrated for 300,000 years the evolution of all the asteroids in the 1997 update of the catalog [E. Bowell, K. Muinonen, L. H. Wasserman, in *Asteroids, Comets, Meteors*, A. Milani, M. DiMartino, A. Cellino, Eds. (Kluwer, Dordrecht, Netherlands, 1994), pp. 477–481] with perihelion distance smaller than 1.78 AU. An asteroid has been categorized as MCA if it passes through the torus defined by heliocentric distance r between 1.341 and 1.706 AU and vertical coordinate $|z| < r \sin(6.4°)$. These bounds account for a martian maximal eccentricity and inclination of 0.12 and 6.4°, respectively. Asteroid diameters have been estimated assuming the albedos reported in Table 1, if IRAS measurements are not available.
6. M. Menichella, P. Paolocchi, P. Farinella, *Earth Moon Planets* **72**, 133 (1996); for a discussion, see also conclusions of (*4*).
7. Numerical integration was done with the swift_rmvs3 numerical integrator [H. Levison and M. Duncan, *Icarus* **108**, 18 (1994)].
8. Proper elements were computed by averaging the orbital elements over a 10-My running window. The initial proper elements are therefore related to the first 10 My of evolution.
9. A detailed analysis of the chaotic structure of the asteroid belt and its relationship with Fig. 2 is reported in A. Morbidelli and D. Nesvorný, *Icarus*, in press. For three-body resonances see D. Nesvorný and A. Morbidelli, *Astron. J.*, in press.
10. About 40% are transported by the 3/1 resonance, 40% by ν_6 resonance or the closely located 4/1 resonance with Jupiter, and 20% by other resonances.
11. This is done by multiplying the number of MCAs larger than 5 km by the fraction of integrated MCAs that are found on ECA orbits as a function of time. We restrict our considerations to asteroids larger than 5 km for which observational biases can be neglected in the first approximation.
12. Secular resonances with the inner planets are important in this phase; see P. Michel and Ch. Froeschlé, *Icarus* **128**, 230 (1997) and P. Michel, *ibid.*, **129**, 348 (1997).
13. The ν_{16} resonance occurs when the mean precession rate of the asteroid's node equals that of Jupiter.
14. In principle, our argument might be circular: If comets' contribution were nonnegligible, we could have underestimated the number of ECAs larger than 5 km by assuming a typical asteroidal albedo. Note, however, that most of the albedos measured for the Near Earth asteroids are in the range considered by us [D. F. Lupishko and M. Di Martino, *Planet. Space Sci.* **46**, 47 (1998)].
15. A. Milani and Z. Knezevic, *Icarus* **107**, 219 (1994).
16. About 10,000, according to R. Jedicke and T. S. Metcalfe [*Icarus* **131**, 245 (1998)]; extrapolating the size distribution of the asteroid families, this number is increased by 50% [V. Zappala and A. Cellino, in *Completing the Inventory of the Solar System, ASP Conf. Series* **107**, 29 (1996)].
17. The Tisserand invariant is related to the relative velocity at encounter between the body and the planet. If the planet is on a circular orbit, the encounter velocity vector is rotated during the encounter, but its norm is preserved [G. Valsecchi and A. Manara, *Astron. Astrophys.* **323**, 986 (1997)].
18. 0.16 for $2.1 \leq a < 2.36$; 0.13 for $2.36 \leq a < 2.48$; 0.14 for $2.48 \leq a < 2.61$; 0.11 for $2.61 \leq a < 2.75$; 0.12 for $2.75 \leq a < 2.80$; 0.10 for $2.80 \leq a < 3.00$.

19. We thank the European Space Agency and the Conseil Général des Alpes Maritimes for postdoctoral grants provided to P. Michel and D. Nesvorný, respectively.

15 June 1998; accepted 23 July 1998